Published in final edited form as:
Mol Genet Metab. 2006 July ; 88(3): 244–255. doi:10.1016/j.ymgme.2006.02.012.

Enhancement of drug delivery to bone: Characterization of human tissue-nonspecific alkaline phosphatase tagged with an acidic oligopeptide

Tatsuo Nishioka[a,b,1], **Shunji Tomatsu**[a,*,1], **Monica A. Gutierrez**[a], **Ken-ichi Miyamoto**[b], **Georgeta G. Trandafirescu**[a], **Patricia L.C. Lopez**[a], **Jeffrey H. Grubb**[c], **Rie Kanai**[d], **Hironori Kobayashi**[d], **Seiji Yamaguchi**[d], **Gary S. Gottesman**[a], **Richard Cahill**[a], **Akihiko Noguchi**[a], and **William S. Sly**[c]

a *Department of Pediatrics, Cardinal Glennon Children's Hospital, Saint Louis University, St. Louis, MO, USA*

b *Department of Hospital Pharmacy, Kanazawa University, Kanazawa, Japan*

c *Department of Biochemistry and Molecular Biology, Saint Louis University School of Medicine, St. Louis, MO, USA*

d *Department of Pediatrics, Shimane University, Shimane, Japan*

Abstract

Hypophosphatasia is caused by deficiency of activity of the tissue-nonspecific alkaline phosphatase (TNSALP), resulting in a defect of bone mineralization. Enzyme replacement therapy (ERT) with partially purified plasma enzyme was attempted but with little clinical improvement. Attaining clinical effectiveness with ERT for hypophosphatasia may require delivering functional TNSALP enzyme to bone. We tagged the C-terminal-anchorless TNSALP enzyme with an acidic oligopeptide (a six or eight residue stretch of L-Asp), and compared the biochemical properties of the purified tagged and untagged enzymes derived from Chinese hamster ovary cell lines. The specific activities of the purified enzymes tagged with the acidic oligopeptide were the same as the untagged enzyme. In vitro affinity experiments showed the tagged enzymes had 30-fold higher affinity for hydroxyapatite than the untagged enzyme. Lectin affinity chromatography for carbohydrate structure showed little difference among the three enzymes. Biodistribution pattern from single infusion of the fluorescence-labeled enzymes into mice showed delayed clearance from the plasma up to 18h post infusion and the amount of tagged enzyme retained in bone was 4-fold greater than that of the untagged enzyme. In vitro mineralization assays with the bone marrow from a hypophosphatasia patient using each of the three enzymes in the presence of high concentrations of pyrophosphate provided evidence of bone mineralization. These results show the anchorless enzymes tagged with an acidic oligopeptide are delivered efficiently to bone and function bioactively in bone mineralization, at least in vitro. They suggest potential advantages for use of these tagged enzymes in ERT for hypophosphatasia, which should be explored.

Keywords

Hypophosphatasia; Drug delivery system; Alkaline phosphatase

*Corresponding author. Fax: +1 3145775398. E-mail address: tomatsus@slu.edu (S. Tomatsu).
[1]The authors wish it to be known that, in their opinion, the first two authors should be regarded as joint first authors.

Introduction

Alkaline phosphatases (ALP) comprise several plasma membrane-bound isozymes, some of which show tissue specific localization. Hypophosphatasia is an inherited metabolic disorder of defective bone mineralization caused by deficiency of the tissue-nonspecific alkaline phosphatase (TNSALP). Clinical severity is remarkably variable, ranging from death in utero to merely premature loss of dentition in adult life [1,2]. Despite the presence of TNSALP in bone, kidney, liver, and adrenal tissue in healthy individuals, clinical manifestations in patients with hypophosphatasia are limited to defective skeletal mineralization that manifests as rickets in infants and children and osteomalacia in adults [2]. In the most pernicious form of hypophosphatasia, the perinatal lethal variant, profound skeletal hypomineralization results in caput membranaceum with shortened and deformed limbs noted. Some affected neonates survive for several days or weeks. They often succumb to respiratory failure brought on by pulmonary hypoplasia and structural failure of the skeleton, weakened from demineralization [3].

Osteoblasts modulate the composition of the bone matrix, where they deposit mineral in the form of hydroxyapatite. Specialized buds from the osteoblasts' plasma membrane are called matrix vesicles (MVs). The initiation of matrix calcification by osteoblasts and chondrocytes appears to be mediated by release of MVs, which serve as a sheltered environment for hydroxyapatite crystal formation [4–7]. MVs are alkaline phosphatase enriched, extracellular, membrane-invested bodies, inside which the first crystals of hydroxyapatite bone mineral are generated. TNSALP hydrolyzes inorganic pyrophosphate (PP_i) to monophosphate (inorganic phosphate; P_i), which is important for growth of the hydroxyapatite crystal [4,5,8–10]. Thus ALP functions as an inorganic pyrophosphatase (PP_i-ase) [14,15]. PP_i itself impairs the growth of hydroxyapatite crystals and acts as an inhibitor of mineralization [8,11–13]. If TNSALP activity is insufficient, it fails to hydrolyze PP_i and the resulting build-up of unhydrolyzed PP_i in the perivesicular matrix inhibits the proliferation of pre-formed hydroxyapatite crystals beyond the protective confines of MV membranes.

The level of plasma PP_i increases in hypophosphatasia [16–18]. Even in the absence of TNSALP, the other phosphatases (AMPase and inorganic pyrophosphatase) can hydrolyze PP_i, supplying some P_i for incorporation into initial mineral within MVs [19], but this activity is insufficient to remove excess PP_i at the perimeter of MVs. Thus, despite TNSALP deficiency, initial mineral could form within MVs, while its propagation into perivesicular matrix would be inhibited by a local build-up of PP_i [20,21]. These findings suggest PP_i as a plausible candidate as an inhibitor of mineralization and as a primary factor that causes clinical manifestations of hypophosphatasia.

Enzyme replacement therapy (ERT) has proven effective in preventing or reversing lysosomal storage in patients and animal models with several lysosomal storage diseases (LSDs) [22–28]. Tremendous progress in the development of ERT has been made in the last three decades. Cellular uptake of enzyme from the blood following intravenous administration requires specific oligosaccharides on the enzyme itself corresponding to oligosaccharide receptors on the target cells. Examples include the binding of high-mannose oligosaccharides of the enzyme to the mannose receptor (MR) and binding of phosphorylated high-mannose oligosaccharides of the enzyme to the cation-independent mannose 6-phosphate receptor (M6PR). Thus, LSDs have provided a prototype for therapy with exogenously supplied enzymes.

A cell-specific delivery system was designed to enhance the clinical effectiveness of ERT in Gaucher disease. Delivery of the enzyme to the affected cells was achieved by modifying the N-linked carbohydrate on the enzyme. This exposed core mannose residues [29,30], enabling the enzyme to bind to the MR, which is highly abundant on cells of the reticuloendothelial

system [31,32], the principal site of storage in Gaucher disease. Over 3500 patients have been treated with dramatic clinical results [22,33].

Moreover, to overcome the limited delivery of an enzyme to a specific tissue, peptide-based targeting strategies have been attempted experimentally by using a lysosomal enzyme, β-glucuronidase [34,35]. LeBowitz et al. fused a portion of IGF-II to this enzyme, retaining the ability to bind to IGF-II receptor, which is present in many mammalian cell types. This fused-enzyme was taken up by cells through an IGF-II receptor-mediated mechanism. Orii et al. also fused the C-terminus portion of Tat HIV protein containing the 11 amino acid transduction domain to (β-glucuronidase. Although neither fusion protein delivered enzyme to brain, distribution to tissues not typically targeted by control enzymes was demonstrated [35].

Since hypophosphatasia is caused by a deficiency of a single enzyme, TNSALP, this disorder is potentially amenable to ERT. The results of ERT, however, with intravenous infusion of plasma ALP or purified liver ALP in patients with hypophosphatasia have been disappointing [36–40]. Recently, one report suggested that continuous delivery of high dose of TNSALP to bone would be needed to induce physiological bone mineralization [41]. These observations suggested that these ALP enzymes administered intravenously are consumed mainly in visceral organs and not delivered to bone at physiologic levels capable of rescuing lesions of the targeted tissue, namely bone. Thus, development of targeted enzyme delivery to bone might enhance clinical effectiveness of the administered ALP. Recently, Kasugai et al. [42] have demonstrated that a small peptide consisting of acidic amino acids (L-Asp or L-Glu) was selectively delivered to and retained in bone after a systemic administration. Furthermore, estrogen conjugated with an acidic oligopeptide was selectively targeted to bone, leading to dramatic improvement of the bone mineral density in ovariectomized mice with no or few adverse effects on liver and uterus [43]. Whether the bone-targeting system with an acidic oligopeptide would be applicable to a large molecule, like the TNSALP enzyme, remains to be determined.

In this study, we characterized acidic oligopeptide-tagged TNSALP enzymes, evaluated the bone-targeting property of these tagged enzymes pharmacokinetically and bioactively, in the hopes of developing a bone-targeting TNSALP as a potential therapeutic agent.

Materials and methods

Production of human recombinant acidic oligopeptide-tagged and untagged TNSALPs (GenBank: NM_000478.2)

The glycosylphosphatidylinositol (GPI) anchoring signal peptide sequence of TNSALP (5′-CTTGCTGCAGGCCCCCTGCTGCTCGCTCTGGCCCTCTACCCCCTGAGCGTCCTGTTC-3′: C.1516C to c.1572 C: Leu506 to Phe524) was deleted from the full-length of TNSALP cDNA to produce a secreted form of the enzyme. To produce acidic oligopeptide-tagged TNSALP, a stretch of six or eight of L-Asp codons (six L-Asp, 5′-GACGATGACGACGATGAT-3′: eight L-Asp, 5′-GATGATGATGATGATGATGACGAC-3′) was introduced additionally at the C-terminus after c.1515C of Ser505 (CD6- or CD8-TNSALP, respectively) between the spacer (5′-ACCGGTGAAGCAGAGGCC-3′) and a termination codon. The three enzymes used for the further experiments were named: rhTNSALP (anchorless recombinant human TNSALP), CD6-TNSALP (anchorless human TNSALP tagged with a stretch of six L-Asp at the C-terminus), and CD8-TNSALP (anchorless human TNSALP tagged with a stretch of eight L-Asp at the C-terminus).

For the preparation of the first strand cDNA, reverse transcriptase reaction was performed by using total RNA isolated from healthy human peripheral blood. To amplify rhTNSALP, CD6-TNSALP, and CD8-TNSALP cDNA, PCR reactions were carried out with the following

primers: TNSALP, forward 5′-GAATTCACCCACGTCGATTGCATCTCTGGGCTCCAG-3′ and reverse 5′-ctcgagTCAGCTGCCTGCCGAGCTGGCAGGAGCAC-3′: CD6-TNSALP, forward 5′-GAATTCACCCACGTCGATTGCATCTCTGGGCTCCAG-3′ and reverse 5′-tcaatcatcgtcgtcatcgtcggcctctgcttcaccggtGCTGCCTGCCGAGCTGGCAGGAGCACAGTG-3′: CD8-TNSALP, forward 5′-GAATTCACCCACGTCGATTGCATCTCTGGGCTCCAG-3′ and reverse 5′-tcagtcgtcatcatcatcatcatcggcctctgcttcaccggtGCTGCCTGCCGAGCTGGCAGGAGCACAGTG-3′. The nucleotide sequences compatible with six or eight L-Asp were added to the reverse primers used here. The amplified cDNAs were cloned and sequenced. The cDNAs were then transferred into *Eco*RI cloning sites of mammalian expression vector pCXN, kindly provided by Miyazaki J., Osaka University, Suita, Japan [44].

The rhTNSALP, CD6-TNSALP, and CD8-TNSALP cDNAs subcloned in pCXN were then transfected into Chinese hamster ovary (CHO-K1) cells with lipofectamine according to manufacturer's instruction (Invitrogen, CA). Selection of colonies was carried out in growth medium with Dulbecco's modified Eagle's medium supplemented with 15% fetal bovine serum (FBS), plus 600 μg/ml G418 (Sigma–Aldrich, MO) for 10–12 days. Individual clones were picked, grown to confluency, and analyzed for enzyme expression by measuring secreted enzyme activity in the medium as described below. The highest-producing clone was grown in collection medium with Ex-Cell tm 325 PF CHO protein-free medium (JRH Biosciences, KS) and 15% FBS. When the cells reached confluency, the cells were rinsed with PBS and fed with collection medium without FBS to collect enzyme for purification.

Measurement of alkaline phosphatase activity

A 50 μl volume of sample was combined with 250 μl of 10 mM *p*-nitrophenyl phosphate (*p*NPP) (Sigma–Aldrich, MO) as a substrate in 1 M diethanolamine, pH 9.8, containing 1 mM magnesium chloride, 0.02 mM zinc chloride, and incubated at 37°C. The time-dependent increase in absorbance at 405 nm (reflecting *p*-nitrophenolate production) was measured on a plate spectrophotometer (EL800, Bio-Tek Instrument, Inc., VT). One unit of activity was defined as the quantity of enzyme that catalyzed the hydrolysis of 1 μmol substrate in 1 min.

Enzyme purification

The rhTNSALP, CD6-TNSALP, and CD8-TNSALP enzymes were purified by a two-step column procedure. Tris buffer was 25 mM Tris–HCl, pH 8.0, containing 0.1 mM magnesium chloride and 0.01 mM zinc chloride. Unless stated otherwise, all steps were performed at 4° C.

Step 1. The medium containing enzyme was filtered through a 0.2 μm filter and then dialyzed against Tris buffer using Amicon stirred-cell ultrafiltration unit with Millipore ultrafiltration membrane YM-30.

Step 2. The dialyzed medium was applied to a column of DEAE-Sepharose (Sigma–Aldrich, MO) equilibrated with Tris buffer. The column was first washed with Tris buffer and then the enzyme was eluted with 0 0.4 M NaCl in a linear gradient.

Step 3. The active eluted fractions were pooled and dialyzed against Tris buffer containing 0.1 M NaCl by using Centricon centrifugal filter device with Millipore ultrafiltration YM-10 filter. The dialyzed fractions were then concentrated for Step 4.

Step 4. The concentrated enzyme was applied to a column of Sephacryl S-400-HR (Sigma–Aldrich, MO) equilibrated with Tris buffer containing 0.1 M NaCl. The enzyme was eluted with Tris buffer containing 0.1 MNaCl.

Step 5. The active eluted fractions were pooled and dialyzed against Tris buffer containing 0.1 M NaCl by using Centricon centrifugal filter device with Millipore ultrafiltration YM-10 filter. The dialyzed fractions were then concentrated and stored at − 80°C until use.

Polyacrylamide gel electrophoresis

Polyacrylamide gel electrophoresis in the presence of sodium dodecyl sulfate (SDS–PAGE) was performed, followed by silver staining [45,46].

Hydroxyapatite-binding assay

Hydroxyapatite beads (Sigma–Aldrich, MO) were suspended in 25 mM Tris–HCl buffered saline (TBS), pH 7.4, at concentration of 100 μg/100 μl. The purified enzyme was mixed with the hydroxyapatite suspension at a final concentration of 1.0, 2.5, 5.0, and 10.0 μg/ml. The mixture was mixed at 37°C for 1 h, and centrifuged at 14,000 × rpm for 10 min to separate the unbound enzyme and the bound enzyme. To determine the unbound enzyme, the enzyme activity in supernatant was measured, and the bound enzyme was determined from the amount of the total enzyme and the unbound enzyme. The dissociation constant (K_d) and the maximal binding rate (B_{max}) were determined from double-reciprocal plots.

Lectin affinity chromatography

To evaluate the carbohydrate chain structure, we analyzed the enzymes by two types of lectin affinity chromatography. Both the concanavalin A (*Canavalia ensiformis*, ConA)-Sepharose 4B (Sigma–Aldrich, MO) and the wheat germ agglutinin (*Triticum vulgaris*, WGA)-agarose CL-4B (Fluka, SG, Switzerland) columns were equilibrated with TBS (10 mM Tris–HCl, pH 8.0, supplemented with 0.5 M sodium chloride, 1 mM calcium chloride, 1 mM magnesium chloride, 1 mM manganese chloride, and 0.01 mM zinc chloride) at a flow rate of 0.2 ml/min. Lectin affinity chromatography was performed as described previously [47]. Briefly, the purified enzyme in 0.6 ml of TBS was applied to the ConA and WGA columns, and left to stand for 3h at room temperature. Three fractions were obtained by using two different concentrations, 0.01 and 0.5 M of α-methyl-D-mannopyranoside (αMM) (Sigma–Aldrich, MO) from ConA column, and 0.1 and 0.5 M of *N*-acetyl-D-glucosamine (GlcNAc) (Sigma–Aldrich, MO) from the WGA column: unbound fraction, weakly bound fraction, and strongly bound fraction.

Neuraminidase digestion

We digested the enzymes with α(2→ 3,6,8,9) neuraminidase (*Arthrobacter ureafaciens*) (Sigma–Aldrich, MO) to quantify the content of sialic acids at the carbohydrate chain. Twenty units of each purified TNSALP enzyme were exposed to 0.01 U neuraminidase in 250 mM sodium phosphate, pH 6.0, overnight at room temperature. The digested enzyme was then analyzed by polyacrylamide gel electrophoresis and lectin affinity chromatography, as described above.

Biodistribution of Alexa-labeled enzymes

Purified enzymes (1 mg/ml) were labeled with Alexa Fluor 546 Protein Labeling Kit following manufacturer's instruction (Molecular Probes, OR). The Alexa-labeled enzyme was injected into B6 mice (6–7-weeks-old) via tail vein at a dose of 1 mg/kg of body weight. Mice were sacrificed at 6, 24, 72, and 168h after a single infusion, and multiple tissues including brain, lung, heart, liver, spleen, kidney, and leg were dissected. The tissues were immersion-fixed in 10% neutral buffered formalin, embedded in paraffin, and sectioned. Tissues were studied by fluorescence microscopy for enzyme distribution, and the areas of fluorescence from three

fields of fluorescent images around the growth plate were quantitated by using Alpha-EaseFC (Alpha Innotech Corp., CA).

In vitro mineralization assay

To evaluate the level of bioactivity of the TNSALP enzymes, in vitro mineralization experiments were performed using bone marrow cells derived from a hypophosphatasia patient with an infantile form (10 month old). The bone marrow was obtained with an informed consent approved by the ethical committee at Shimane University. The bone marrow cells were seeded into 150 × 25 mm tissue culture dishes. These cells were allowed to attach without disturbance for seven days in growth medium consisting of minimum essential medium alpha (MEMα) supplemented with 10% FBS, 50U/ml penicillin, and 50 μg/ml streptomycin sulfate. The medium was then replaced to fresh growth medium at 3-day intervals. When the cells reached confluency, they were subcultured in the 12-well plates at a density of 10,000 cells/cm^2. On the following day, the growth medium was replaced with the differentiation medium: with MEMα supplemented with 10% FBS, 50 U/ml penicillin, 50 μg/ml streptomycin sulfate, 0.3 mM ascorbic acid, and 100nM dexamethasone. The differentiation medium also included 2.5 mM P_i or β-glycerophosphate as a phosphate source as well as either rhTNSALP, CD6-TNSALP, or CD8-TNSALP at 2.5 or 5.0 U/ml. To further investigate the effect of the three enzymes on mineralization in the presence of PP_i, 50 μM PP_i was always added with each enzyme to the bone marrow cell culture throughout the differentiation period.

The differentiation medium was replaced at 3-day intervals. At 12 days after the initiation of the differentiation of the cells, the cells were fixed with 4% paraformaldehyde, followed by staining with Alizarin Red S to detect calcium phosphate deposits [48].

Results

Preparation and biochemical characterization of enzymes

The GPI anchoring signal peptide (19 amino acids) sequence was removed from the C-terminus of the human TNSALP cDNA to allow secretion of the enzyme in the medium of CHO-K1 cells. The resultant rhTNSALP enzyme (>95%) was primarily secreted in culture medium in a transient expression study (Fig. 1A). The acidic oligopeptide-tagged enzymes (CD6-TNSALP and CD8-TNSALP), which also do not include the GPI anchoring signal peptide, were secreted into culture medium as well. Other results showed that the presence of greater than eight Asp residues caused substantial reduction of the enzyme activity secreted into culture medium during the transient expression. Therefore, we chose the CD6- and CD8-TNSALP enzymes for further experiments. The stably transfected CHO-K1 cells secreted the active TNSALP enzyme into the medium in linear fashion for 12h. However, the expression of enzyme after 12h reached a plateau.

The purification of these enzymes from secretion media of stably transfected cells was performed by two-step column chromatography using DEAE-Sepharose and Sephacryl S-400-HR, and summarized in Table 1. The overall purification yield of rhTNSALP, CD6-TNSALP, and CD8-TNSALP was 32, 62, and 56% of the total enzyme in the initial culture medium, respectively, and the specific activity of each enzyme was 2744, 2411, and 2374 U/mg, respectively. The lower yield of rhTNSALP compared to those of the tagged enzymes was apparently the result of the broader peak eluted from the DEAE column. When the purified rhTNSALP was subjected to SDS–PAGE under reducing conditions, a single band with a molecular mass of approximately 80kDa was detected. The anticipated increase in molecular mass associated with the addition of acidic oligopeptides was observed with CD6- and CD8-TNSALP(Fig. 1B).

There was no significant difference in the Michaelis constant (K_M) among rhTNSALP, CD6-TNSALP, and CD8-TNSALP defined by the *p*NPP substrate with double-reciprocal plots (0.37, 0.39, and 0.37 mM, respectively) (Table 2). The values of k_{cat} among three enzymes showed little difference as well. Similarly, chemical inhibition by L-phenylalanine (10mM; 83, 86, and 86% of remaining enzyme activity, respectively) and L-homoarginine (10mM; 12, 13, and 12% of remaining enzyme activity, respectively) revealed no significant difference.

In contrast, remarkable differences were observed between the tagged and untagged enzymes in their affinity for hydroxyapatite. The affinity for hydroxyapatite for the tagged enzymes was 30-fold greater than that for the untagged enzyme. The binding to hydroxyapatite was seen even at low concentrations of the tagged enzyme (Fig. 2). The binding parameters, K_d and B_{max}, are shown in Table 3. The values of K_d and B_{max} of the tagged enzymes were 30-fold and 3-fold, respectively, greater than those of the untagged enzymes, although no significant difference was observed between CD6- and CD8-TNSALP.

Elution profiles of enzymes by lectin affinity chromatography

The three enzymes, rhTNSALP, CD6-, and CD8-TNSALP were applied to ConA columns. The ConA column bound nearly all of the applied enzymes, but the weakly bound and strongly bound enzymes were differentiated by the concentration of α-acetate, which eluted them. The elution profiles of these enzymes did not differ when the two different concentrations of αMM, the competitive sugars, were added (Fig. 3). We concluded that these three enzymes did not differ with respect to exposed mannosyl residues with which ConA has a high reactivity. In contrast, the WGA elution profiles between the tagged and untagged enzymes were remarkably different with regard to the ratio of strongly bound enzyme and weakly bound enzyme (Fig. 4A, a–c). Table 4 shows the percentages of the relative enzyme activity of three fractions on the WGA column. By contrast, approximately 30% of the tagged enzymes was weakly bound and 70% was strongly bound to the WGA column, and 66% of the untagged enzyme was weakly bound and 34% was strongly bound to the WGA column. The content of the weakly bound enzyme fractions ranged from greatest to least in the order of TNSALP >CD6-TNSALP > CD8-TNSALP. This suggests a greater fraction of the wild-type TNSALP contains fewer sialic acid complex chain oligosaccharides.

To evaluate the content of the sialic acid residues of the enzyme, we treated the three enzymes with neuraminidase, removing the sialic acid residues from the enzymes. After the treatment with neuraminidase, the molecular masses of the three enzymes decreased in different proportion (Fig. 4B). The elution profile of the untagged enzyme on the WGA column changed after the neuraminidase digestion. The early fraction, accounting for the weakly bound enzyme, shifted to a later fraction consistent with the highly bound enzyme (Fig. 4A, d). The elution profiles of the tagged enzymes on the WGA column showed a similar change after neuraminidase digestion (Fig. 4A, e and f), but the tagged enzymes originally included a smaller amount of weakly bound enzyme.

Biodistribution of fluorescence-labeled enzymes

To evaluate the pharmacokinetic tissue distribution pattern of the enzymes, fluorescence-labeled enzymes were prepared with Alexa dye. The efficiencies of labeling each of three enzymes were approximately 10mol/mol of protein as dye content. Fig. 5A shows the histological pictures of biodistribution of three enzymes at the proximal epiphyseal region of mouse femur at 6, 24, 72, and 168h after a single intravenous infusion. Fig. 5B shows the average of the relative area of fluorescence. The three enzymes were distributed in the mineralized region, but not at the growth plate. At 6 h, the relative areas of fluorescence of the tagged enzymes were 4-fold larger than the area of the untagged enzyme. Moreover, the fluorescence-labeled tagged enzymes were detectable until 168h with a 2- to 3-fold increase

compared to the untagged enzyme. These results were consistent with the result of the in vitro hydroxyapatite affinity experiment. A relatively high level of enzyme was distributed in the liver (Fig. 6) compared to the other tissues. The distribution was widespread throughout the liver including hepatocytes and sinus-lining cells. The distribution patterns in the liver were comparable among three enzymes. In the other tissues, including brain, lung, heart, spleen, and kidney, no significant differences were observed among three enzymes (data not shown).

Effect of control and tagged enzymes on mineralization in the presence of PP_i in primary bone marrow cell culture

We had the opportunity to ask whether the tagged enzymes enhance mineralization in the presence of PP_i in primary bone culture. The effect of normal TNSALP has been reported previously. We found that the addition of one of the tagged enzymes resulted in marked recovery of mineralization like that seen with the untagged enzyme (data not shown). Mineralization was observed when P_i, was used in the medium instead of β-glycerophosphate even in the absence of any enzyme. In the presence of P_i, none of the enzymes provided any additive effect on mineralization. These findings indicate that like the TNSALP enzyme, the tagged enzyme can play a biological role in the mineralization process in vitro by providing free P_i released during the hydrolysis of β-glycerophosphate. We added *PP_i*, an inhibitor of mineralization, to see whether the TNSALP enzymes hydrolyze PP_i to restore the mineralization. In the absence of added TNSALP, PP_i itself completely inhibited the mineralization even in the presence of P_i. The addition of the tagged enzymes restored the mineralization level to PP_i free control culture as had been reported for TNSALP (data not shown). Taken together, these results suggested that the tagged and untagged enzymes show similar bioactivity on mineralization by degrading PP_i.

Overall, we found no biochemical or pharmacokinetic differences between the CD6 and CD8 forms of tagged TNSALP.

Discussion

This study demonstrated that: (1) the removal of the GPI anchoring signal peptide sequence at the C-terminus of TNSALP cDNA allowed us to produce large amounts of human recombinant enzyme in a secreted form: (2) tagging an oligopeptide of six or eight L-Asp to the C-terminus of rhTNSALP enhanced the affinity of rhTNSALP for hydroxyapatite with little influence on other biochemical properties; (3) the tagged rhTNSALP enzymes were delivered more efficiently to and retained longer in bone; and (4) the tagged enzymes were bioactive in vitro and able to initialize bone mineralization in cultured bone marrow from a hypophosphatasia patient.

In vivo, the TNSALP is bound to plasma membranes by the GPI anchor and functions as an ectoenzyme. In this study, we removed the GPI anchoring signal peptide coding sequence from human TNSALP cDNA in order to produce an anchorless secretory form of TNSALP in the culture medium of overexpressing CHO-K1 cells. As a consequence, sufficient human recombinant enzyme could be obtained for additional studies. The CD6- and CD8-TNSALP enzymes possess biochemical properties similar to the rhTNSALP with regard to specific activity, in vitro bioactivity, kinetic parameters, heat stability, and chemical inhibition, suggesting that the acidic oligopeptide tag did not markedly affect any functions of the alkaline phosphatase, at least in vitro. These findings are similar to those in a previous report, where the biochemical properties of wild-type GPI-anchored TNSALP were compared to those of enzyme containing an eight amino acid FLAG epitope at the C-terminal of the enzyme [49]. However, the acidic oligopeptide-tagged TNSALP showed markedly higher affinity for hydroxyapatite compared to the untagged TNSALP. This high affinity for hydroxyapatite

resulted in more efficient delivery of tagged enzymes to bone. Hydroxyapatite is produced in extracellular matrix near osteoblasts and is one of the major components of bone [42,43].

TNSALP is a glycoprotein with potential glycosylation sites. Little is known about the physiological role of specific carbohydrate structures present in the ALP isoenzymes except that a. larger sialic acid residue content at the terminus of the carbohydrate chain contributes to longer half-lives of ALP in the blood circulation [50–52]. Thus, an analysis of the carbohydrate structure, especially the enzyme's sialic acid content, may be important for estimation of the efficiency of bone-targeting. Enzyme circulating longer in blood may reasonably have more opportunity to reach bone. We observed a difference in the elution profile of the three enzyme variants on the WGA affinity chromatography, when these enzymes were eluted by two different concentrations of GlcNAc. Specifically, the percentage of the enzyme bound weakly to the column varied from greatest to least in the order of rhTNSALP >CD6-TNSALP>CD8-TNSALP. After neuraminidase digestion, the enzymes which had bound weakly to the WGA column were retained more strongly. Both GlcNAc and sialic acid residues bind to WGA, although sialic acid residues are more weakly bound than GlcNAc residues [53]. Gallagher et al. demonstrated WGA binds with high affinity to internal GlcNAc residues in large oligosaccharides containing repeat sequence of Galβ(1 → 4)GlcNAcβ(1 → 3) (polylactosamine-type glycans), and with low affinity to sialic acid-dependent binding [54].

The lectin binding results suggest that the untagged TNSALP is more highly sialylated. The three recombinant TNSALP enzymes used here showed no M6P-receptor-mediated uptake, indicating that the enzymes were not phosphorylated (data not shown). Therefore, this study indicates that all three enzymes produced by CHO-K1 cells have internal polylactosamine-type glycans as well as a substantial amount of sialic acid. Interestingly, these findings differ from those of human TNSALP from osteosarcoma cells, where the affinity of human bone TNSALP isoenzyme to WGA was largely lost after neuraminidase treatment, suggesting that human TNSALP from osteosarcoma cells has few polylactosamine-type glycans [55]. The effect on in vivo function of the alkaline phosphatase caused by abundance of internal GlcNAc residues will require additional study.

Based on our present data, we propose that there are three possibilities for carbohydrate structure related to the sialic acid content in the three enzyme variants: (1) the acidic oligopeptide-tagged enzymes have fewer sialic acid residues than the untagged enzyme as indicated by a lower percentage of the weakly bound enzyme observed during the WGA affinity chromatography; (2) the tagged enzymes have similar sialic acid residue content to the untagged enzyme but larger internal polylactosamine-type glycans. This conclusion is supported by the similar proportional reduction of molecular mass of the three enzymes after the neuraminidase digestion and the higher percentage of the strongly bound enzyme during WGA affinity chromatography; and (3) the tagged enzymes include a slightly decreased amount of sialic acid and increased content of internal polylactosamine-type glycans. The enzymes have slightly different half-lives in circulation (rhTNSALP, 19.1h; CD6-TNSALP, 14.4h; and CD8-TNSALP, 13.5h) after a single intravenous infusion (Fig. 7).

The next question we addressed is whether the tagged enzymes could be targeted more efficiently to bone. We have demonstrated that more of each tagged enzyme was retained longer compared to the untagged enzyme in the mineralized region close to growth plate, where physiological mineralization is initiated. The distribution to other tissues was not significantly different among the three enzymes. In vitro bone mineralization experiments with the bone marrow cells from a hypophosphatasia patient indicated that the tagged TNSALP enzymes are functionally active, like the untagged enzymes in the presence of PP_i levels, and enhance mineralization at the cellular level.

ERT is an established strategy for treating LSDs and is clinically available or in clinical trials for Gaucher disease [22], Fabry disease [28], Pompe disease [56], MPS I [26], MPS II, and MPS VI. Those ERTs result in marked improvement in the visceral organs but little improvement in the bone and the brain since the enzymes are not delivered effectively to these tissues. Initial ERT attempts at clinical trials on patients with hypophosphatasia were conducted in early 1980s, before the cloning of the TNSALP gene, by using plasma from the patients with Paget disease. These produced discouraging results [36]. The potential reasons for the unsatisfactory outcome were: (1) the TNSALP present in administered plasma was not delivered adequately to bone sufficiently to metabolize the high level of PP_i to normal physiologic levels locally; and/or (2) the TNSALP administered did not function as native ALP in bone.

The potential of selective drug delivery to target tissues has stimulated significant biochemical inquiry because it can enhance clinical efficacy, reduce pathology and limit a drug's side effects in other tissues. Positively charged hydroxyapatite is a major inorganic component of bone and is not present in soft tissues. Bone is remodeled by a cycle of resorption and formation throughout life. Therefore, a drug absorbed by hydroxyapatite in the bone, may be released in the bone resorption process. Such targeting of the drug to hydroxyapatite could be a potential strategy for a selective drug delivery to the bone [57,58]. Moreover, some bone matrix proteins (osteopontin, bone sialoprotein, etc.) that bind to hydroxyapatite have been found to have a repetitive sequence of negatively charged acidic amino acids (Asp or Glu), a possible hydroxyapatite-binding site [34,59]. In osteoblast cell culture, osteopontin and bone sialoprotein rapidly bind to hydroxyapatite after the osteoblasts secrete these proteins [60]. Kasugai et al. showed that oligopeptides containing six residues of L-Asp (Asp_6 or D_6) could be localized specifically in bone by administering D_6 conjugated with fluorescein isothiocyanate intravenously to mice. The first therapeutic candidate was osteoporosis, the most common metabolic bone disorder, characterized by microarchitectural deterioration of bone tissue leading to enhanced bone fragility and an increase in fracture risk. The L-Asp homopeptides consisting of two to ten residues were conjugated with estradiol and the binding affinity of each L-Asp homopeptide to hydroxyapatite was investigated. The results showed that estradiol tagged with D_6 is bone-specific compared to estradiol. The uptake level in soft tissues was less than in estradiol. Thus, estradiol with at least six residues of L-Asp was observed to prevent bone loss in ovariectomized (osteoporosis) mice without causing liver damage or increasing uterine weight [61]. Bone density improved with fewer adverse effects, suggesting that estradiol tagged with the acidic oligopeptide is a potential drug to treat a postmenopausal osteoporosis [43]. These results indicated the usefulness of tagging a drug with six or more acidic amino acids in order to more effectively deliver the drug to bone with bioactivity at least in vitro.

In conclusion, this study provides important new information on the acidic oligopeptide-tagging strategy designed to deliver a large molecule, like an enzyme, to bone and suggests the possible clinical application of ERT for hypophosphatasia. Further studies are needed to prove that these tagged enzymes are physiologically functional in vivo. We demonstrated bioactivity by the in vitro mineralization experiment, and have determined the optimal number of L-Asp to tag to TNSALP. The established hypophosphatasia mouse model [62,63] should provide a great opportunity to evaluate the clinical effectiveness of ERT through the use of tagged and untagged recombinant enzymes.

Acknowledgements

This work was supported by grants from the Austrian Research Society for Mucopolysaccharidoses and Related Diseases, German MPS, International Morquio Organization, Italian MPS Society, the Jacob Randall Foundation, the Bennett Foundation, and National Institutes of Health Grant GM34182 to W.S.S.

References

1. Fraser D. Hypophosphatasia. Am J Med 1957;22:730–746. [PubMed: 13410963]
2. Whyte, MP. Hypophosphatasia. In: Scriver, CR.; Beaudet, AL.; Sly, WS.; Valle, D., editors. The Metabolic and Molecular Bases of Inherited Disease. 8. McGraw-Hill; New York: 2001. p. 5313-5329.
3. Silver MM, Vilos GA, Milne KJ. Pulmonary hypophosphatasia in neonatal hypophosphatasia. Pediatr Pathol 1988;8:483–493. [PubMed: 3227000]
4. Ali, SY. Matrix formation and mineralization in bone. In: Whitehead, CC., editor. Bone Biology and Skeletal Disorders. Carfax Publishing Co.; Abingdon, UK: 1992. p. 19-38.
5. Anderson HC. Molecular biology of matrix vesicles. Clin Orthop Relat Res 1995;314:266–280. [PubMed: 7634645]
6. Boskey AL, Boyan BD, Schwartz Z. Matrix vesicles promote mineralization in a gelatin gel. Calcif Tissue Int 1997;60:309–315. [PubMed: 9069171]
7. Boskey AL. Amorphous calcium phosphate: the contention of bone. J Dent Res 1997;76:1433–1436. [PubMed: 9240379]
8. Anderson HC. Mechanisms of pathologic calcification. Rheum Dis Clin North Am 1988;14:303–319. [PubMed: 2845491]
9. Bonewald LF, Schwartz Z, Swain LD, Boyan BD. Stimulation of matrix vesicle enzyme activity in osteoblast-like cells by 1.25(OH)2D3 and transforming growth factor beta (TGFβ). Bone Miner 1992;17:139–144. [PubMed: 1611299]
10. Fedde KN. Human osteosarcoma cells spontaneously release matrix-vesicle-like structures with the capacity to mineralize. Bone Miner 1992;17:145–151. [PubMed: 1611300]
11. Fleisch H, Russell RG, Straumann F. Effect of pyrophosphate on hydroxyapatite and its implications in calcium homeostasis. Nature 1966;212:901–903.
12. de Jong AS, Hak TJ, van Duijn P. The dynamics of calcium phosphate precipitation studied with a new polyacrylamide steady state matrix-model: influence of pyrophosphate collagen and chondroitin sulfate. Connect Tissue Res 1980;7:73–79. [PubMed: 6244132]
13. Meyer JL. Can biological calcification occur in the presence of pyrophosphate? Arch Biochem Biophys 1984;15:1–8. [PubMed: 6326671]
14. Moss DW, Eaton RH, Smith JK, Whitby LG. Association of inorganic-pyrophosphatase activity with human alkaline-phosphatase preparations. Biochem J 1967;102:53–57. [PubMed: 6030299]
15. Leon FA, Rezende LA, Ciancaglini P, Pizauro JM. Allosteric modulation of pyrophosphatase activity of rat osseous plate alkaline phosphatase by magnesium ions. Int J Biochem Cell Biol 1998;30:89–97. [PubMed: 9597756]
16. Russell RG, Bisaz S, Donath A, Morgan DB, Fleisch H. Inorganic pyrophosphate in plasma in normal persons and in patients with hypophosphatasia, osteogenesis imperfecta, and other disorders of bone. J Clin Invest 1971;50:961–965. [PubMed: 4324072]
17. Sorensen E, Flodgaard H. Adult hypophosphatasia. Acta Med Scand 1975;197:357–360. [PubMed: 167553]
18. Sorensen SA, Flodgaard H, Sorensen E. Serum alkaline phosphatase, serum pyrophosphatase, phosphorylethanolamine and inorganic pyrophosphate in plasma and urine. A genetic and clinical study of hypophosphatasia. Monogr Hum Genet 1978;10:66–69. [PubMed: 214699]
19. Anderson HC. Pyrophosphate stimulation of calcium uptake into cultured embryonic bones. Fine structure of matrix vesicles and their role in calcification. Dev Biol 1973;34:211–227. [PubMed: 4363671]
20. Anderson HC, Hsu HH, Morris DC, Fedde KN, Whyte MP. Matrix vesicles in osteomalacic hypophosphatasia bone contain apatite-like mineral crystals. Am J Pathol 1997;151:1555–1561. [PubMed: 9403706]
21. Anderson HC, Sipe JB, Hessle L, Dhanyamraju R, Atti E, Camacho NP, Millan JL. Impaired calcification around matrix vesicles of growth plate and bone in alkaline phosphatase-deficient mice. Am J Pathol 2004;164:841–847. [PubMed: 14982838]
22. Barton NW, Brady RO, Dambrosia JM, Di Bisceglie AM, Doppelt SH, Hill SC, Mankin HJ, Murray GJ, Parker RI, Argoff CE, et al. Replacement therapy for inherited enzyme deliciency-macro-phage-

targeted glucocerebrosidase for Gaucher's disease. N Engl J Med 1991;324:1464–1470. [PubMed: 2023606]

23. Sands MS, Vogler C, Kyle JW, Grubb JH, Levy B, Galvin N, Sly WS, Birkenmeier EH. Enzyme replacement therapy for murine mucopolysaccharidosis type VII. J Clin Invest 1994;93:2324–2331. [PubMed: 8200966]
24. Shull RM, Kakkis ED, McEntee MF, Kania SA, Jonas AJ, Neufeld EF. Enzyme replacement in a canine model of Hurler syndrome. Proc Natl Acad Sci USA 1994;91:12937–12941. [PubMed: 7809150]
25. Crawley AC, Brooks DA, Muller VJ, Petersen BA, Isaac EL, Bielicki J, King BM, Boulter CD, Moore AJ, Fazzalari NL, Anson DS, Byers S, Hopwood JJ. Enzyme replacement therapy in a feline model of Maroteaux-Lamy syndrome. J Clin Invest 1996;97:1864–1873. [PubMed: 8621770]
26. Kakkis ED, Muenzer J, Tiller GE, Waber L, Belmont J, Passage M, Izykowski B, Phillips J, Doroshow R, Walot I, Hoft R, Neufeld EF. Enzyme-replacement therapy in mucopolysaccharidosis I. N Engl J Med 2001;344:182–188. [PubMed: 11172140]
27. Altarescu G, Hill S, Wiggs E, Jeffries N, Kreps C, Parker CC, Brady RO, Barton NW, Schiffmann R. The efficacy of enzyme replacement therapy in patients with chronic neuronopathic Gaucher's disease. J Pediatr 2001;138:539–547. [PubMed: 11295718]
28. Eng CM, Guffon N, Wilcox WR, Germain DP, Lee P, Waldek S, Caplan L, Linthorst GE, Desnick RJ. International collaborative Fabry disease study group, safety and efficacy of recombinant human α-galactosidase A-replacement therapy in Fabry's disease. N Engl J Med 2001;345:9–16. [PubMed: 11439963]
29. Furbish FS, Steer CJ, Krett NL, Barranger JA. Uptake and distribution of placental glucocerebrosidase in rat hepatic cells and effects of sequential deglycosylation. Biochim Biophys Acta 1981;673:425–434. [PubMed: 6784774]
30. Murray GJ. Lectin-specific targeting of lysosomal enzymes to reticuloendothelial cells. Methods Enzymol 1987;149:25–42. [PubMed: 3695962]
31. Stahl PO, Rodman JS, Miller MJ, Schlesinger PH. Evidence for receptor-mediated binding of glycoproteins. glycoconjugates, and glycosidases by alveolar macrophages. Proc Natl Acad Sci USA 1978;75:1399–1403. [PubMed: 274729]
32. Achord DT, Brot FE, Bell CE, Sly WS. Human β-glucuronidase: in vivo clearance and in vitro uptake by a glycoprotein recognition system on reticuloendothelial cells. Cell 1978;15:269–278. [PubMed: 699046]
33. Barranger JA, O'Rourke E. Lessons learned from the development of enzyme therapy for Gaucher disease. J Inherit Metab Dis 2001;24:89–96. [PubMed: 11758684]
34. LeBowitz JH, Grubb JH, Maga JA, Schmiel DH, Vogler C, Sly WS. Glycosylation-independent targeting enhances enzyme delivery to lysosomes and decreases storage in mucopolysaccharidosis type VII mice. Proc Natl Acad Sci USA 2004;101:3083–3088. [PubMed: 14976248]
35. Orii KO, Grubb JH, Vogler C, Levy B, Tan Y, Markova K, Davidson BL, Mao Q, Orii T, Kondo N, Sly WS. Defining the pathway for Tat-mediated delivery of β-glucuronidase in cultured cells and MPS VII mice. Mol Ther 2005;12:345–352. [PubMed: 16043103]
36. Whyte MP, Valdes R, Ryan LM, McAlister WH. Infantile hypophosphatasia: enzyme replacement therapy by intravenous infusion of alkaline phosphatase-rich plasma from patients with Paget bone disease. J Pediatr 1982;101:379–386. [PubMed: 7108657]
37. Whyte MP, McAlister WH, Patton LS, Magill HL, Fallon MD, Lorentz WB, Herrod HG. Enzyme replacement therapy for infantile hypophosphatasia attempted by intravenous infusions of alkaline phosphatase-rich Paget plasma: results in three additional patients. J Pediatr 1984;105:926–933. [PubMed: 6502342]
38. Whyte MP, Magill HL, Fallon MD, Herrod HG. Infantile hypophosphatasia: normalization of circulating bone alkaline phosphatase activity followed by skeletal remineralization. Evidence for an intact structural gene for tissue nonspecific alkaline phosphatase. J Pediatr 1986;108:82–88. [PubMed: 3944698]
39. Weninger M, Stinson RA, Plenk H, Böck P, Pollak A. Biochemical and morphological effects of human hepatic alkaline phosphatase in a neonate with hypophosphatasia. Acta Paediatr Scand Suppl 1989;360:154–160. [PubMed: 2642253]

40. Whyte MP, Landt M, Ryan LM, Mulivor RA, Henthorn PS, Fedde KN, Mahuren JD, Coburn SP. Alkaline phosphatase: placental and tissue-nonspecific isoenzymes hydrolyze phosphoethanolamine, inorganic pyrophosphatem and pyridoxal 5′-phosphate. Substrate accumulation in carriers of hypophosphatasia corrects during pregnancy. J Clin Invest 1995;95:1440–1445. [PubMed: 7706447]
41. Murshed M, Harmey D, Millan JL, McKee MD, Karsenty G. Unique coexpression in osteoblasts of broadly expressed genes accounts for the spatial restriction of ECM mineralization to bone. Genes Dev 2005;19:1093–1104. [PubMed: 15833911]
42. Kasugai S, Fujisawa R, Waki Y, Miyamoto K, Ohya K. Selective drug delivery system to bone: small peptide (Asp)6 conjugation. J Bone Miner Res 2000;15:936–943. [PubMed: 10804024]
43. Yokogawa K, Miya K, Sekido T, Higashi Y, Nomura M, Fujisawa R, Morito K, Masamune Y, Waki Y, Kasugai S, Miyamoto K. Selective delivery of estradiol to bone by aspartic acid oligopeptide and its effects on ovariectomized mice. Endocrinology 2001;142:1228–1233. [PubMed: 11181539]
44. Niwa H, Yamamura K, Miyazaki J. Efficient selection for high-expression transfectants with a novel eukaryotic vector. Gene 1991;15:193–199. [PubMed: 1660837]
45. Laemmli UK. Cleavage of structural proteins during the assembly of the head of bacteriophage T4. Nature 1970;227:680–685. [PubMed: 5432063]
46. Merril CR, Goldman D, Van Keuren ML. Silver staining methods for polyacrylamide gel electrophoresis. Methods Enzymol 1983;96:230–239. [PubMed: 6197605]
47. Koyama I, Sakagishi Y, Komoda YT. Different lectin affinities in rat alkaline phosphatase isozymes: multiple forms of the isozyme isolated by heterogeneities of sugar moieties. J Chromatogr 1986;374:51–59. [PubMed: 3081567]
48. Mcgee-Russell SM. Histochemical methods for calcium. J Histochem Cytochem 1958;6:22–42. [PubMed: 13514045]
49. Di Mauro S, Manes T, Hessle L, Kozlenkov A, Pizauro JM, Hoylaerts MF, Millan JL. Kinetic characterization of hypophosphatasia mutations with physiological substrates. J Bone Miner Res 2002;17:1383–1391. [PubMed: 12162492]
50. Komoda T, Sakagishi Y. The function of carbohydrate moiety and alteration of carbohydrate composition in human alkaline phosphatase isoenzymes. Biochim Biophys Acta 1978;523:395–406. [PubMed: 656434]
51. Walton RJ, Preston CJ, Russell RG, Kanis JA. An estimate of the turnover rate of bone-derived plasma alkaline phosphatase in Paget's disease. Clin Chim Acta 1975;63:227–229. [PubMed: 1175295]
52. Clubb JS, Neale FC, Posen S. The behavior of infused human placental alkaline phosphatase in human subjects. J Lab Clin Med 1965;66:493–507. [PubMed: 5835974]
53. Bhavanandan VP, Katlic AW. The interaction of wheat germ agglutinin with sialoglycoproteins. The role of sialic acid. J Biol Chem 1979;254:4000–4008. [PubMed: 108267]
54. Gallagher JT, Morris A, Dexter TM. Identification of two binding sites for wheat-germ agglutinin on polylactosamine-type oligosaccharides. Biochem J 1985;231:115–122. [PubMed: 3840682]
55. Magnusson P, Farley JR. Differences in sialic acid residues among bone alkaline phosphatase isoforms: a physical, biochemical, and immunological characterization. Calcif Tissue Int 2002;71:508–518. [PubMed: 12232676]
56. Van den Hout JM, Kamphoven JH, Winkel LP, Arts WF, De Klerk JB, Loonen MC, Vulto AG, Cromme-Dijkhuis A, Weisglas-Kuperus N, Hop W, Van Hirtum H, Van Diggelen OP, Boer M, Kroos MA, Van Doorn PA, Van der Voort E, Sibbles B, Van Corven EJ, Brakenhoff JP, Van Hove J, Smeitink JA, de Jong G, Reuser AJ, Van der Ploeg AT. Long-term intravenous treatment of Pompe disease with recombinant human α-glucosidase from milk. Pediatrics 2004;113:e448–e457. [PubMed: 15121988]
57. Butler WT. The nature and significance of osteopontin. Connect Tissue Res 1989;23:123–136. [PubMed: 2698313]
58. Fujisaki J, Tokunaga Y, Takahashi T, Shimojo F, Kimura S, Hata T. Osteotropic drug delivery system (ODDS) based on bisphosphonic prodrug. iv effects of osteotropic estradiol on bone mineral density and uterine weight in ovariectomized rats. J Drug Target 1998;5:129–138. [PubMed: 9588869]
59. Oldberg A, Franzen A, Heinegard D. Cloning and sequence analysis of rat bone sialoprotein (osteopontin) cDNA reveals an Arg-Gly-Asp cell-binding sequence. Proc Natl Acad Sci USA 1986;83:8819–8823. [PubMed: 3024151]

60. Nagata T, Bellows CG, Kasugai S, Butler WT, Sodek J. Biosynthesis of bone proteins [SPP-1 (secreted phosphoprotein-1, osteopontin), BSP (bone sialoprotein) and SPARC (osteonectin)] in association with mineralized-tissue formation by fetal-rat calvarial cells in culture. Biochem J 1991;274:513–520. [PubMed: 2006915]

61. Sekido T, Sakura N, Higashi Y, Miya K, Nitta Y, Nomura M, Sawanishi H, Morito K, Masamune Y, Kasugai S, Yokogawa K, Miyamoto K. Novel drug delivery system to bone using acidic oligopeptide: pharmacokinetic characteristics and pharmacological potential. J Drug Target 2001;9:111–121. [PubMed: 11697106]

62. Waymire KG, Mahuren JD, Jaje JM, Guilarte TR, Coburn SP, MacGregor GR. Mice lacking tissue non-specific alkaline phosphatase die from seizures due to defective metabolism of vitamin B-6. Nat Genet 1995;11:45–51. [PubMed: 7550313]

63. Narisawa S, Frohlander N, Millan JL. Inactivation of two mouse alkaline phosphatase genes and establishment of a model of infantile hypophosphatasia. Dev Dyn 1997;208:432–446. [PubMed: 9056646]

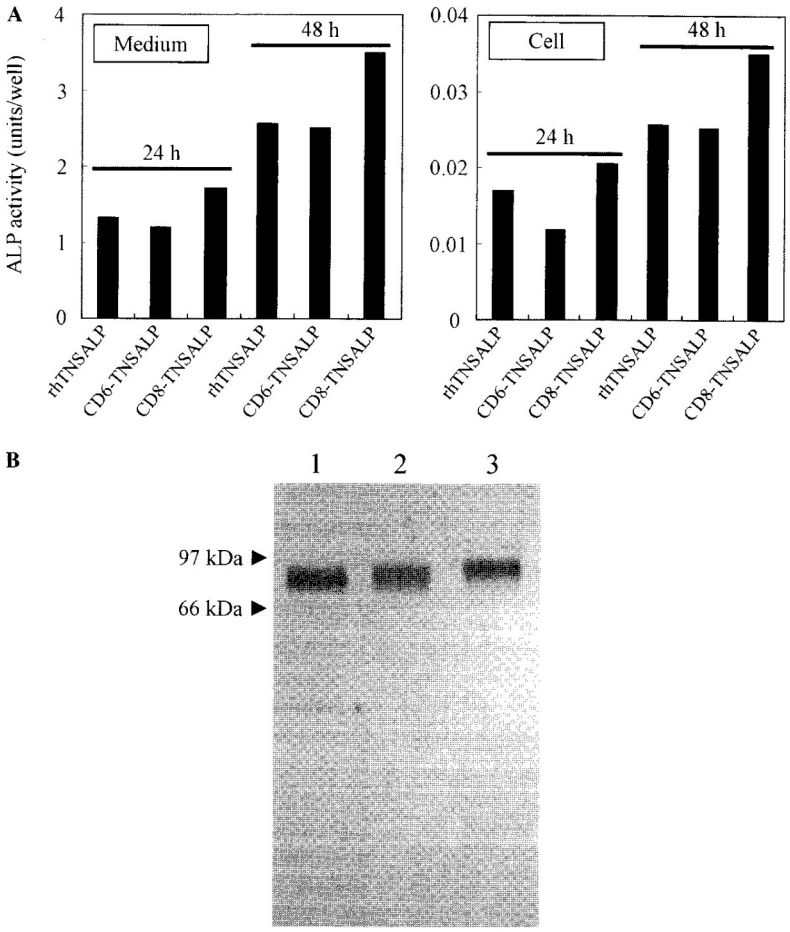

Fig. 1.

Transient expression of rhTNSALP, CD6-TNSALP, and CD8-TNSALP and SDS–PAGE of the purified enzymes. (A) The cDNA of each enzyme subcloned in pCXN vector was transfected into CHO-K1 cells with lipofectamine. At 24 and 48h after transfection, the culture medium and cells were separately collected, and the enzyme activity was determined. (B) The purified enzymes (0.2 μg) were subjected to SDS–PAGE under reducing condition and stained with silver. A single band appeared in all the three enzymes. The molecular mass of the untagged rhTNSALP (lane 1) was approximately 80 kDa, while those of CD6- and CD8-TNSALP were larger (lanes 2 and 3, respectively).

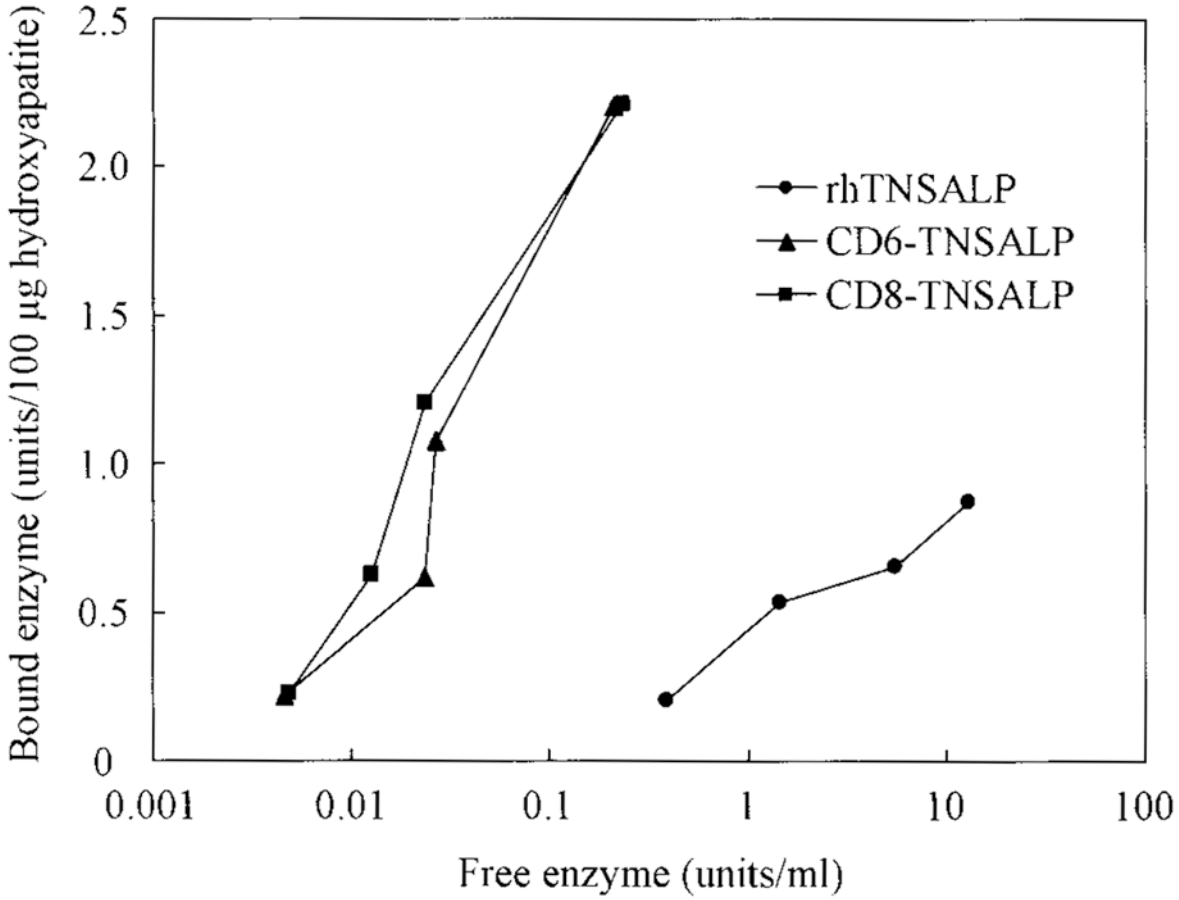

Fig. 2.

Concentration-dependent binding curves of the three enzymes to hydroxyapatite. The purified enzyme was mixed with the hydroxyapatite suspension at a final concentration of 1.0, 2.5, 5.0, and 10.0µg/ml. The mixture was mixed at 37°C for 1 h, and centrifuged at 14,000× rpm for 10 min to separate the unbound and bound enzymes. To determine the amount of the unbound enzyme, the enzyme activity in supernatant was measured, and the amount of the bound enzyme was determined from the amount of both total and unbound enzymes. The affinity to hydroxyapatite for the tagged enzymes was 30-fold higher than that for the untagged enzyme and the binding to hydroxyapatite was seen even at low concentration of the tagged enzyme.

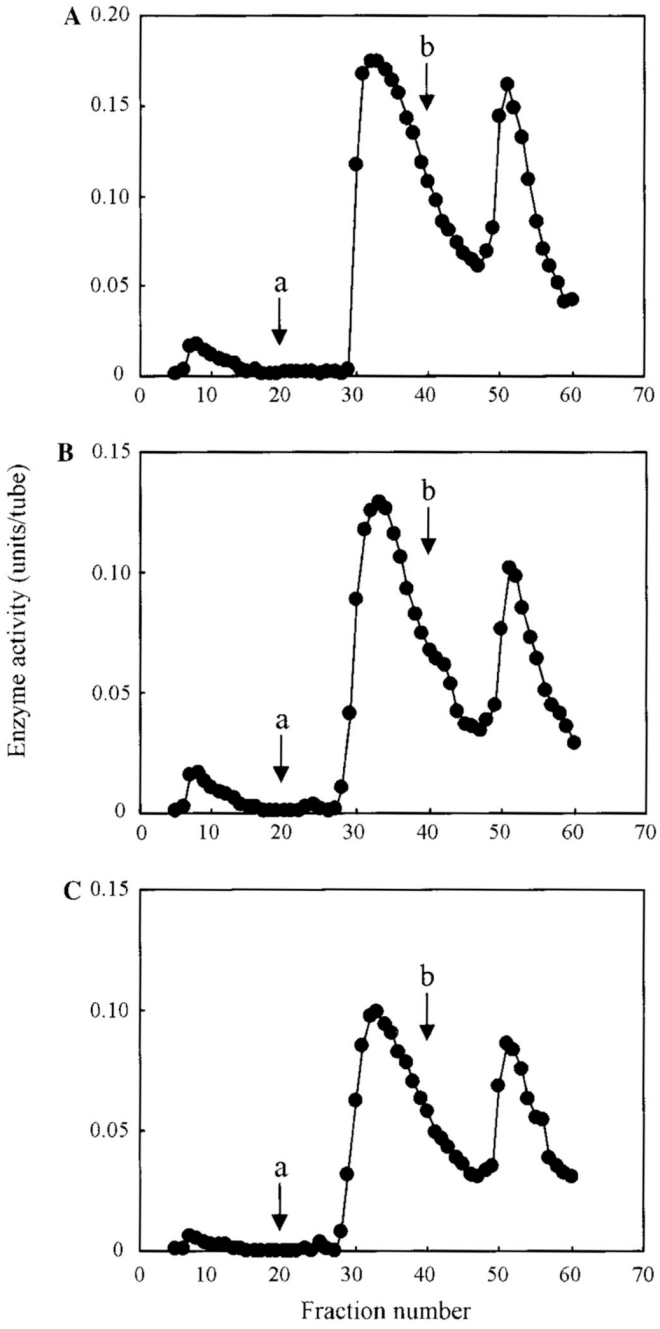

Fig. 3.

ConA affinity chromatography of the three enzymes. The rhTNSALP (A), CD6-TNSALP (B), and CD8 TNSALP (C) enzymes were applied to the ConA column. After washing the column, two fractions were eluted by the two different concentrations, 0.01 M (arrow; a) and 0.5 M (arrow; b) of αMM. There was no difference in the elution profile among the three enzymes.

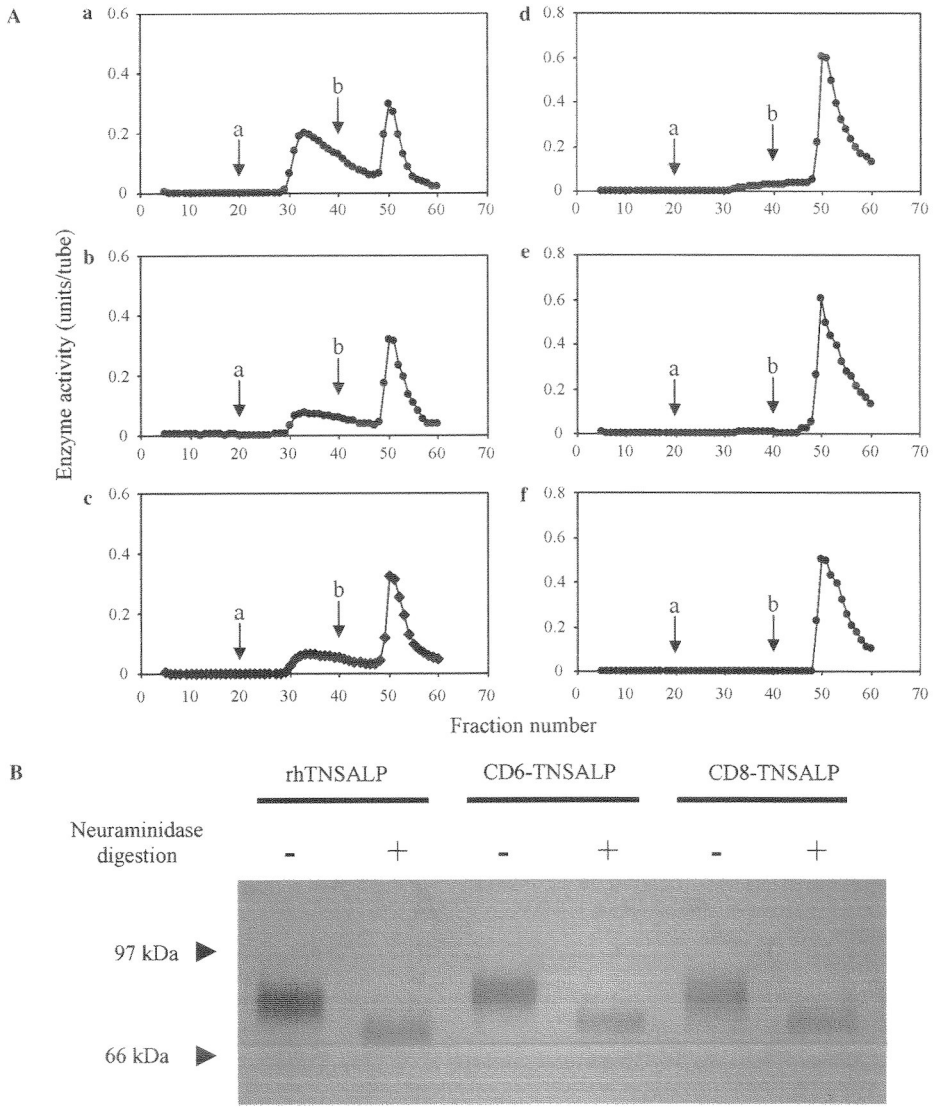

Fig. 4.

WGA affinity chromatography and SDS –PAGE of three enzymes before and after neuraminidasc digestion. (A) Three enzymes before (a –c) and after (d–f) neuraminidase digestion were applied to the WGA affinity chromatography. The rhTNSALP (a and d), CD6-TNSALP (b and e), and CD8-TNSALP (c and f) enzymes were applied to the WGA column. After washing the column, two fractions were eluted by the two different concentrations. 0.1 M (arrow; a) and 0.5 M (arrow; b) of GlcNAc. (B) The enzymes (0.3 μg) were subjected to SDS –PAGE under reducing condition and stained with silver. A single band was observed at all the lanes. After the treatment with neuraminidase, the molecular mass of the three enzymes decreased in a similar proportion.

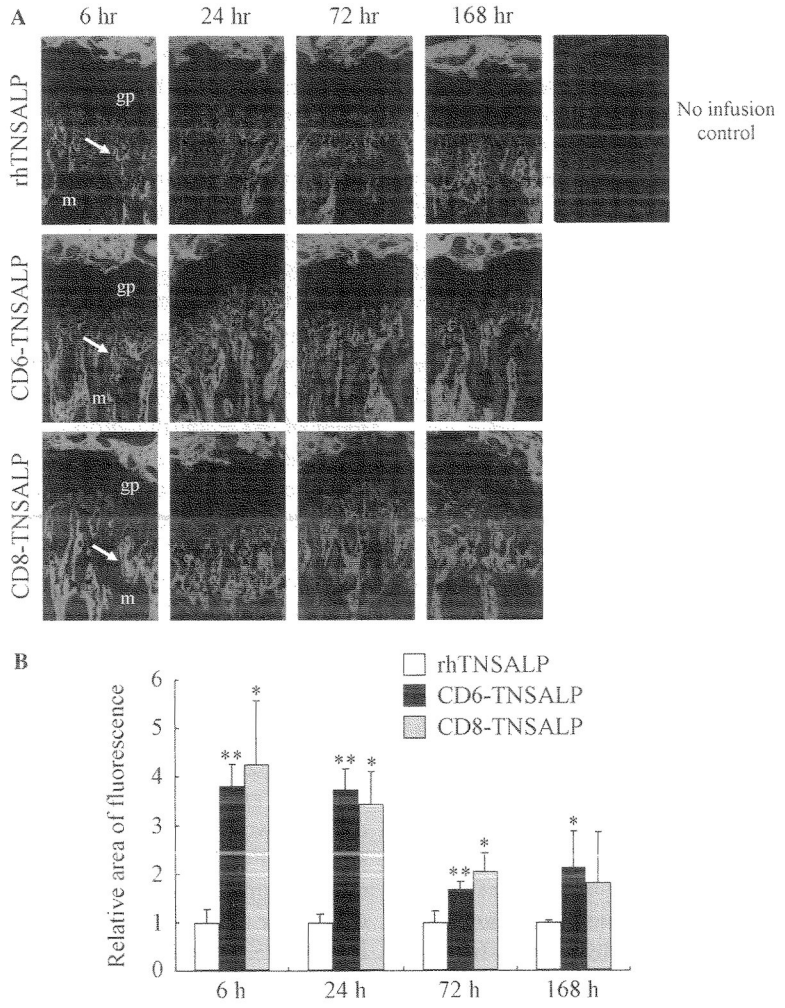

Fig. 5.

Biodistribution of fluorescence-labeled enzyme to bone. The three fluorescence-labeled enzymes were infused into mice by tail vein injections at a dose of 1 mg/kg of body weight. At the indicated time points, the legs were dissected and sectioned. The sections of legs were observed under a fluorescent microscopy to evaluate the enzyme distribution at the epiphyseal region. Three enzymes were distributed to the mineralized region, but not to the growth plate, gp, growth plate; m, mineralized region (A). The average of the relative areas of fluorescence from three fields of the fluorescent images at epiphyseal region was quantitated. $*p < 0.05$ in comparison with the untagged enzyme. $**p < 0.01$ in comparison with the untagged enzyme (B).

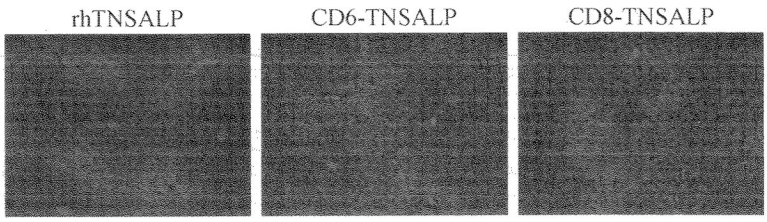

Fig. 6.

Biodistribution of fluorescence-labeled enzyme to liver. The fluorescence-labeled three enzymes were infused to mice from tail vein at the dose of 1 mg/kg of body weight. At 6 h after the infusion, the livers were dissected and sectioned. The sections of legs were observed under a fluorescent microscopy. The distribution patterns in these tissues were comparable among three enzymes.

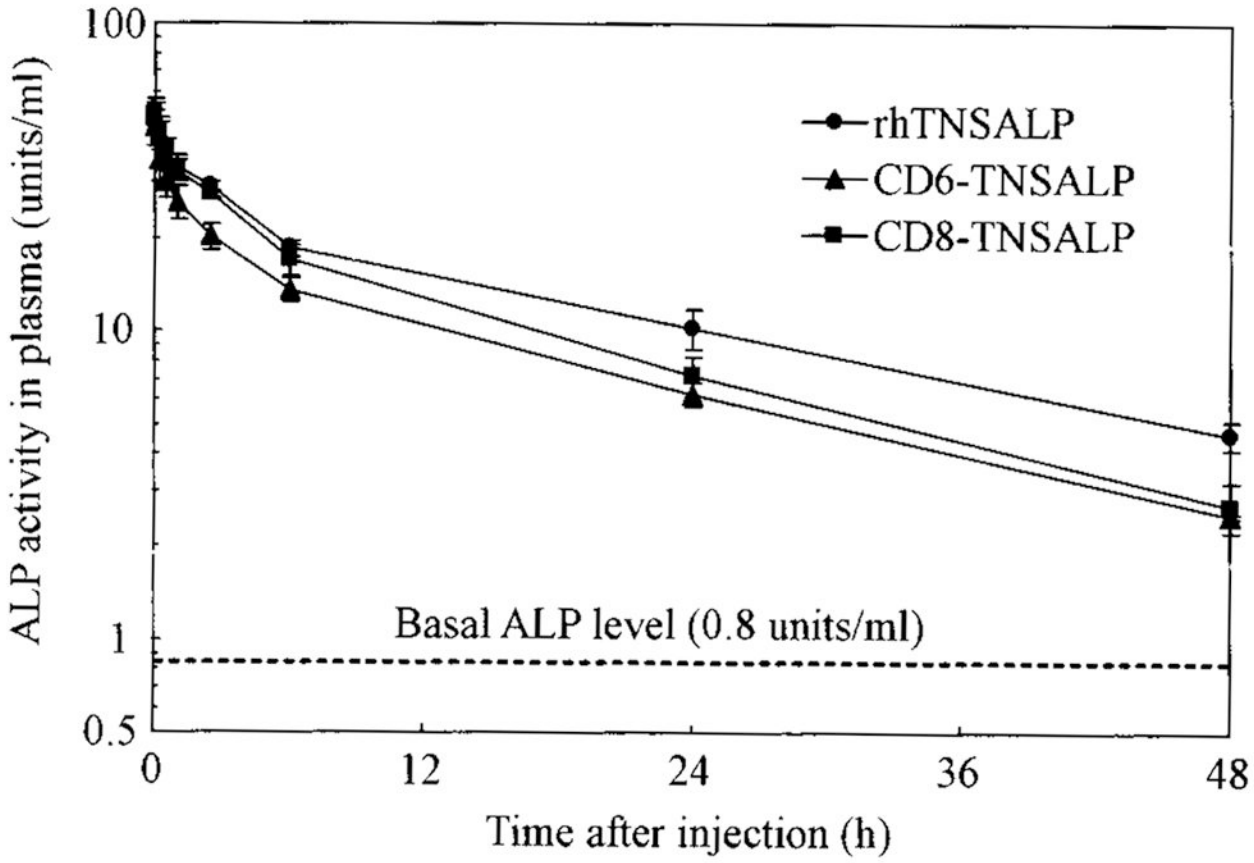

Fig. 7.

Blood clearance of rhTNSALP, CD6-TNSALP, and CD8-TNSALP. The three purified enzymes were intravenously administered to 1-month-old mice at a dose of 2 U/g body weight. Plasma was obtained from infraorbital vein at the indicated time points, and the remaining enzyme activities in plasma were determined.

Table 1

Purification of rhTNSALP and acidic oligopeptide-tagged TNSALP from condition medium

	Protein conc. (mg/l)	Total protein (mg)	Total enzyme activity (U)	Specific activity (U/mg)	Purification	Yield (%)
rhTNSALP						
Crude media	5.26	115	3003	26.1	1	100
DEAE column	18.3	0.66	1555	2354	90	52
Sephacryl S-400-HR column	15.4	0.35	973	2744	105	32
CD6-TNSALP						
Crude media	6.27	127	3022	23.9	1	100
DEAE column	32.3	1.01	2073	2043	86	69
Sephacryl S-400-HR column	22.1	0.77	1862	2411	101	62
CD8- TNSALP						
Crude media	3.85	184	3065	16.6	1	100
DEAE column	29.1	1.00	2028	2035	123	66
Sephacryl S-400-HR column	22.4	0.72	1702	2374	143	56

Table 2

Kinetic parameters and stability properties of three enzymes

	K_M (mM)	Half-life at 56 °C (min)	L-Homoarginine (% of remaining)	L-Phenylalamine (% of remaining)	$k_{cat}(s^{-1})$
rhTNSALP	0.37	15.8	11.6	82.9	2248
CD6-TNSALP	0.39	16.2	12.5	86.2	2874
CD8-TNSALP	0.37	16.6	12.1	86.0	2796

Measurements were done using *p*NPP as substrate chemical inhibitors (L-homoarginine and L-phenylalanine) were used at 10 mM of final concentration.

Table 3

Binding parameters of three enzymes to hydroxyapatite

	K_d (U/ml)	B_{max} (U/100 μg hydroxyapatite)
rhTNSALP	1.66 ± 0.86	1.0 ± 0.3
CD6-TNSALP	0.059 ± 0.017	3.3 ± 0.8
CD8-TNSALP	0.044 ± 0.005	3.4 ± 0.9

Each value represents means ± SD of three experiments. K_d, dissociation constant, and B_{max}, maximal binding rate, were determined from double-reciprocal plots.

Table 4

Percentage of each fraction obtained by each ConA and WGA column

Fractions	Percentage of relative activities								
	ConA			WGA			WGA + Neuraminidase		
	rhTNSALP	CD6-TNSALP	CD8-TNSALP	rhTNSALP	CD6-TNSALP	CD8-TNSALP	rhTNSALP	CD6-TNSALP	CD8-TNSALP
Unbound	3	4	2	0	2	1	0	0	0
Weakly bound	59	60	59	61	35	33	9	1	0
Strongly bound	38	36	39	39	62	66	91	98	99

The percentages were determined from Figs. 3 and 4.